

## 微波还原氧化石墨烯及其气体储存性能研究

随东 黄毅\* 黄璐 张昳 陈永胜\*

(功能高分子材料教育部重点实验室; 天津化学化工协同创新中心; 纳米科学与技术中心;  
高分子化学研究所, 南开大学化学学院, 天津 300071)

**摘要** 通过微波辅助还原氧化石墨烯(GO)的方法, 制备了多孔石墨烯材料(MWRGO), 并对该材料的结构与性质进行了深入研究。结果表明, 微波辐射使得GO有效还原, 还原产物具有多孔、不规则堆积的结构, 其比表面积达 $461.6\text{ m}^2/\text{g}$ , 孔径主要分布在0.67 nm左右。进一步的研究表明, MWRGO材料具有很好的气体储存性能。在77 K一个大气压下, MWRGO可储存0.52 wt%的H<sub>2</sub>, 当压力增加到60 bar时, H<sub>2</sub>储存量高达10.7 wt%; 在273 K一个大气压下, 其对CO<sub>2</sub>的吸附量高达7.1 wt%。

**关键词** 石墨烯; 碳材料; 气体吸附; 微波还原; 多孔材料

## Investigation of Gas Storage Properties of Graphene Material Prepared by Microwave-assisted Reduction of Graphene Oxide

Sui, Dong Huang, Yi\* Huang, Lu Zhang, Yi Chen, Yongsheng\*

(Key Laboratory of Functional Polymer Materials, Collaborative Innovation Center of Chemical Science and Engineering (Tianjin), Center for Nanoscale Science and Technology, Institute of Polymer Chemistry, College of Chemistry, Nankai University, Weijin Road 94, Tianjin 300071, China)

**Abstract** Porous graphene material, named as MWRGO, has been prepared by microwave-assisted reduction method. Extensive characterizations indicate that graphene oxide was effectively reduced and MWRGO has a porous and disordered stacking structure. It has a special surface area of  $461.6\text{ m}^2/\text{g}$  with pore size centered at 0.67 nm. H<sub>2</sub> and CO<sub>2</sub> adsorption properties of MWRGO were investigated, showing a H<sub>2</sub> uptake of 0.52 wt% at 77 K and 1 atm and an absolute adsorption amount as high as 10.7 wt% at a higher pressure of 60 bar. The amount of CO<sub>2</sub> adsorption at 273 K and 1 atm is 7.1 wt%.

**Keywords** graphene; carbon materials; gas storage; microwave reduction; porous materials

## 1 Introduction

Energy crisis, climate change and environmental pollution have been motivating both scientific and industry communities to look for new energy sources to replace traditional fossil fuels which account for the biggest part of world energy consumption and cause lots of CO<sub>2</sub> emission after burned. H<sub>2</sub>, an efficient, sustainable and environmentally friendly alternative and having already found commercial applications in nickel-metal hydride batteries and fuel cells, is attracting increasing attention. However, the most troublesome issue unsolved regarding H<sub>2</sub> usage is storage. Several approaches, including physical storage by compression or liquefaction, chemical storage in irreversible hydrogen carriers and in reversible chemical or metal hydrides, and gas-on-solid adsorption with porous materials, have been proposed to store H<sub>2</sub> for application in motor vehicle.<sup>[1]</sup> Though, unfortunately, every approach has some problems concerning safety, cost, reversibility and efficiency, gas-on-solid adsorption, an inherently safe and

energy efficient method of H<sub>2</sub> storage, has been proved to be an excellent option. What's more, excessive emission of CO<sub>2</sub> causes another worldwide pressing issue—global warming, posing a real threat to the whole world.<sup>[2]</sup> Therefore, it is of great importance to find effective ways to store CO<sub>2</sub>. At present, a few chemical or physical methods, like cryogenic distillation, chilling and pressurizing the exhaust gas, absorption with aqueous amine or ammonia solution, and membrane separation, are commercially used or proposed to capture and store CO<sub>2</sub>, but these means are always costly, toxic, inefficient and energy intensive.<sup>[2-5]</sup> Again, gas-on-solid adsorption, a reversible sorption process with porous materials, is emerging as the most promising method for CO<sub>2</sub> storage. Currently, many porous materials including metal organic frameworks (MOF),<sup>[6]</sup> porous polymer networks,<sup>[7]</sup> and inorganic/organic hybrid material<sup>[8]</sup> have been intensively investigated to store H<sub>2</sub> or CO<sub>2</sub>. Carbon-based porous materials, especially materials with nano-sized structure like single-walled carbon nanotubes,<sup>[9]</sup> zeolite-like carbon,<sup>[10,11]</sup> graphite nanofibers,<sup>[3,12]</sup>

\* E-mail: yihuang@nankai.edu.cn (Huang, Y.), yschen99@nankai.edu.cn (Chen, Y.-S.) Fax: 0086-022-23500693

Received February 12, 2014; published February 25, 2014.

Supporting information for this article is available free of charge via the Internet at <http://sioc-journal.cn>

Project supported by Ministry of Science and Technology of China (Nos. 2012CB933401, 2011CB932602, 2011DFB50300) and Natural Science Foundation of China (Nos. 50933003, 50902073, 50903044).

项目受国家科技部(Nos. 2012CB933401, 2011CB932602, 2011DFB50300)及国家自然科学基金(Nos. 50933003, 50902073, 50903044)资助。

and activated carbons,<sup>[13,14]</sup> have been intensively investigated as H<sub>2</sub> or/and CO<sub>2</sub> adsorbents because of their merits associated with low cost, low mass density, high chemical stability, sufficient availability of raw materials, adjustable pore size and structure, and versatile chemical modification of pore walls and surface. Although exciting results have been achieved, in order for effective H<sub>2</sub> and CO<sub>2</sub> storage, there is still a long way to go to fulfill all the requirements of commercial applications.<sup>[4,15]</sup> Innovative materials, which have high uptake capacity under technologically acceptable conditions and can be manufactured on a large scale, are highly wanted.

Graphene, an amazing 2-D material, possesses many excellent properties,<sup>[16,17]</sup> and has found a wide range of potential applications in optoelectronics,<sup>[18]</sup> energy conversion and storage,<sup>[19-21]</sup> and multifunctional devices.<sup>[22-24]</sup> In addition to all the merits of carbon materials, graphene has a theoretical specific surface area (SSA) as high as 2630 m<sup>2</sup>/g,<sup>[17]</sup> which makes it an ideal gas storage material, especially for H<sub>2</sub> adsorption. Graphene-based materials show significant theoretical H<sub>2</sub> storage capacity at ambient conditions,<sup>[25-29]</sup> and though results still fail to meet all the requirements of commercial applications, recent investigations confirm that graphene and its derivatives are excellent candidates for gas storage.<sup>[30-36]</sup>

Microwave (MW) irradiation is an efficient, green and selective heating method, and has been successfully applied in organic synthesis,<sup>[37]</sup> functionalization of carbon nanotube<sup>[38]</sup> and preparation of exfoliated graphite.<sup>[39]</sup> Recently, MW has been employed to reduce graphene oxide (GO) in solvent<sup>[40]</sup> or under dry condition.<sup>[41]</sup> Furthermore, graphene-based material obtained by MW-assisted reduction has a porous and loose structure and relatively high special surface area,<sup>[41]</sup> making it perfectly suitable for gas storage.

But, so far, there is no such report yet about gas storage of graphene-based porous materials prepared by MW irradiation. Here we employed this time-saved, solvent-free, nontoxic and large-scale method to reduce GO and investigated the gas storage capacity of the obtained material. Microwave-assisted reduction of graphene oxide (MWRGO) possesses a Brunauer-Emmett-Teller (BET) surface area of 461.6 m<sup>2</sup>/g with pore size centered at 0.67 nm. It shows a moderate H<sub>2</sub> uptake of 0.52 wt% at 77 K and 1 atm while an absolute adsorption up to 10.7 wt% is obtained at 60 bar. It also shows high CO<sub>2</sub> uptake of 7.1 wt% at 273 K and 1 atm. These results indicate that this porous graphene material, prepared easily at large scale, could be a highly promising adsorbent for gas storage.

## 2 Results and discussion

### 2.1 Structure of the MWRGO

GO was efficiently reduced to MWRGO by MW irradiation and the color changed from brown to black. The reduction process involves the removal of oxygen-containing functional groups, which was confirmed by the following characterizations. Firstly, the structure changes due to MW treatment can be observed in FTIR spectra, as shown in Figure 1(a). The characteristic IR spectrum of GO are the absorption bands corresponding to the C=O

carbonyl stretching at 1734 cm<sup>-1</sup>, the C—OH stretching at 1226 cm<sup>-1</sup>, the C—O stretching at 1055 cm<sup>-1</sup>, and a controversial absorption at around 1623 cm<sup>-1</sup>.<sup>[42]</sup> But all the corresponding peaks in MWRGO either disappear or become rather weak after MW treatment while an absorption at 1629 cm<sup>-1</sup> related to C=C stretching vibration becomes relatively stronger. Elemental analysis and XPS results further confirm the considerable removal of oxygen-containing functional groups. Elemental analysis shows the molar ratio of C/O increases from 1.64 for GO to 11.36 for MWRGO, which is comparable to that of graphene reduced by hydrazine hydrate.<sup>[43]</sup> As demonstrated in Figure 1(b), the deconvolution of C1s peak in the XPS spectrum of GO shows two signals concerning oxygen-containing groups at 286.4 eV (C—O) and 287.4 eV (C=O), both of which become very weak in the spectrum of MWRGO. Raman is a powerful means to reflect the structure changes of carbon-based materials. As shown in Figure 1(c), compared with GO, both D band and G band for MWRGO are broadened and blue shifted by several wave numbers in addition to an increase of  $I_D/I_G$  intensity ratio (see Supporting Information (SI), Table SI-1). Furthermore, MWRGO has a much depressed 2D band. All of these features demonstrate that MWRGO possesses smaller average sp<sup>2</sup> domain size than that of GO.<sup>[43]</sup> TGA was applied to compare the thermal stability between MWRGO and GO (Figure 1(d)). While GO losses over 40 wt% even below 250 °C, MWRGO, with aromatic structure recovering, shows only 5 wt% loss below 100 °C attributed to residual oxygen functional groups and no more significant loss until 440 °C.

### 2.2 Morphology of MWRGO

The morphology of MWRGO was studied by TEM and SEM. After MW treatment, a fluffy structure and disordered stacking can be observed in Figure 2(a), while GO shows a compact state (see SI, Figure S-2(a)). This is because gases (CO<sub>2</sub>, CO, H<sub>2</sub>O) induced by the MW reduction in very short time created high pressure between layers. As shown in Figure 2(b), compared to a relative planar surface of GO (see SI, Figure S-2(b)) MWRGO shows a wrinkled surface which is a favorable structure for H<sub>2</sub> adsorption.<sup>[44]</sup> Such significant morphology difference between GO and MWRGO in structure is also reflected in their powder XRD patterns in Figure 3. GO shows a typical peak at about  $2\theta=12.2^\circ$  corresponding to an interlayer spacing value of 0.72 nm. In contrary, MWRGO has a rather broad reflection between 15° and 40°, corresponding to a maximum interlayer spacing value of 0.59 nm, with no clear characteristic peak, which is similar to graphene prepared by thermal exfoliation of graphene oxide.<sup>[45]</sup> This indicates that MW assistant heating did remove most of the functional groups and rendered a smaller inter-layer spacing with very disordered stacking.

### 2.3 Gas storage of MWRGO

Figure 4 shows nitrogen adsorption-desorption isotherm of MWRGO. The adsorption isotherm, with a hysteresis loop in the  $P/P_0$  range of 0.45~1.0 which is typical for plate-like materials, exhibits Type I+Type II behavior, demonstrates that MWRGO contains microporous, mesoporous and macroporous structures.<sup>[45-47]</sup> MWRGO

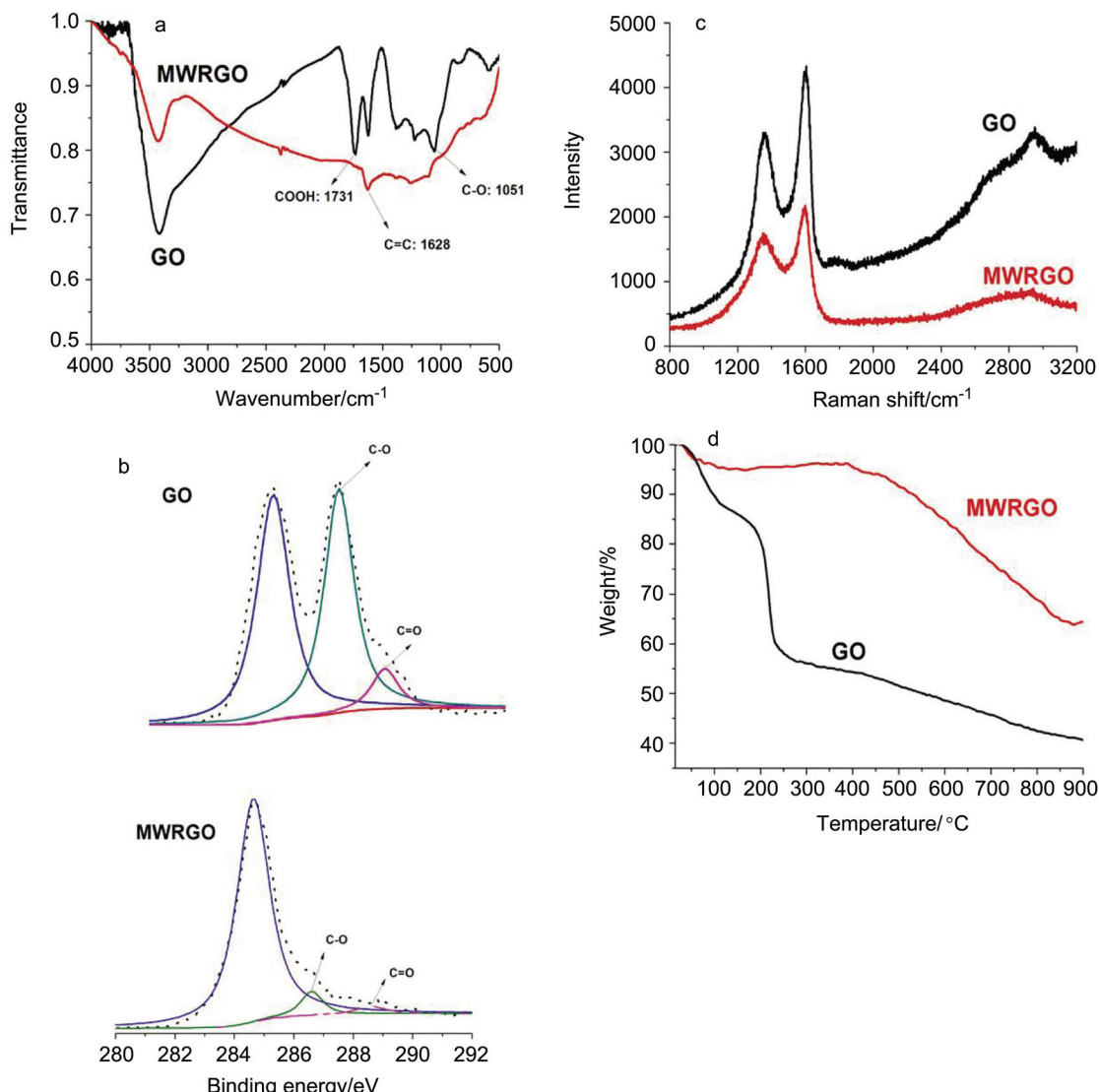


**Figure 1** (a) FTIR, (b) XPS, (c) Raman shift, and (d) TG analysis of GO and MWRGO

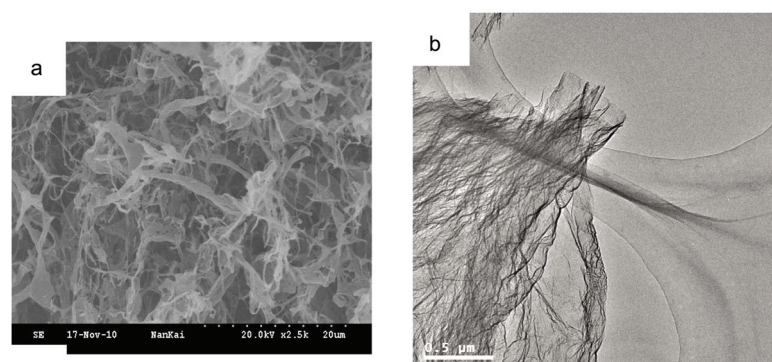


**Figure 2** Typical (a) SEM and (b) TEM images of MWRGO

has a specific surface area of  $461.6 \text{ m}^2/\text{g}$  according to Brunauer-Emmett-Teller method based on the adsorption data in the relative pressure ( $P/P_0$ ) range of 0.05 to 0.3, which is comparable to that of graphene-based materials prepared by other methods,<sup>[41,43]</sup> but still much lower than the theoretical value of ideal graphene.<sup>[17]</sup> Pore size distri-

bution was obtained according to Horvath-Kawazoe method.<sup>[48]</sup> As shown in the inset of Figure 4, MWRGO has both micropores and mesopores while the pore size mainly centered at 0.67 nm, which is proper for  $\text{H}_2$  adsorption.<sup>[25,49]</sup>

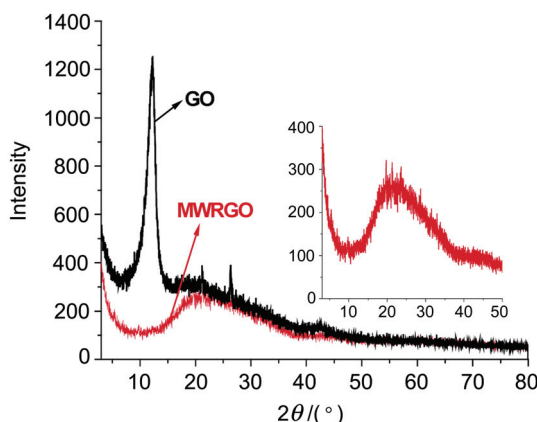


**Figure 3** XRD patterns of GO and MWRGO (inset: a partial enlarged plot of MWRGO)

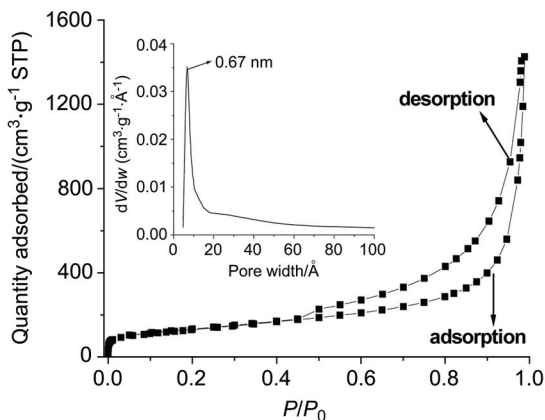


**Figure 4**  $\text{N}_2$  adsorption and desorption isotherm of MWRGO at standard temperature and pressure (STP), (inset: pore size distribution)

Considering its relatively high surface area and proper pore size,  $\text{H}_2$  and  $\text{CO}_2$  adsorption capacity of MWRGO was investigated. Prior to each adsorption/desorption measurement, the experimental setup was evacuated to  $<10^{-2}$  Pa, and carbon sample was heated at 125 °C for 12 h or longer. After the temperature of the sample cell became constant at the investigation condition, the adsorption measurement was started. A high purity hydrogen ( $>99.999\%$ ) was used for hydrogen storage study. Hydrogen storage was determined accumulatively by exposing the sample stepwise to different pressures up to the predicted pressure. Figure 5(a) demonstrates the  $\text{H}_2$  adsorption-desorption isotherms at 77 and 87 K with pressure up to 900 mmHg. Hysteresis loops are observed which may be due to the presence of different sizes and shapes of pores or due to surface heterogeneity.<sup>[31]</sup> MWRGO has a moderate  $\text{H}_2$  uptake of 0.52 wt% at 77 K and 1 atm, which is decreased to 0.42 wt% at 87 K. The isosteric heat ( $Q_{st}$ ) of adsorption was calculated from the adsorption isotherms at different temperatures with Clausius-Clapeyron equation to evaluate the interaction between MWRGO and  $\text{H}_2$ . As shown in Figure 5(b), the  $Q_{st}$  is about 5.1 kJ/mol at low coverage, which is close to theoretical calculation<sup>[50]</sup> and superior to results reported by other group.<sup>[32]</sup> Strong

interaction between  $\text{H}_2$  and MWRGO, resulting from proper pore size, contributes to the exciting value.<sup>[25,49]</sup> But a significant decrease was observed at higher  $\text{H}_2$  uptake, indicating that MWRGO has different sorption sites with different binding energies and multiple adsorption exists.<sup>[32]</sup> The hydrogen uptake was measured by the gravimetric method at 77 and 298 K over the pressure range 1~60 bar. As demonstrated in Figure 6, absolute  $\text{H}_2$  uptake of 10.7 wt% was obtained at 77 K and 60 bar (Figure 6(a)), which is comparable or superior to other materials at similar conditions.<sup>[51,52]</sup> As the temperature increases to 298 K, the absolute adsorption amount decreases rapidly at the same pressure. For example, it becomes 1.26 wt% at 60 bar pressure (Figure 6(b)). Considering the relatively low specific surface area, these results are rather encouraging compared to other carbon-based materials.<sup>[51]</sup>

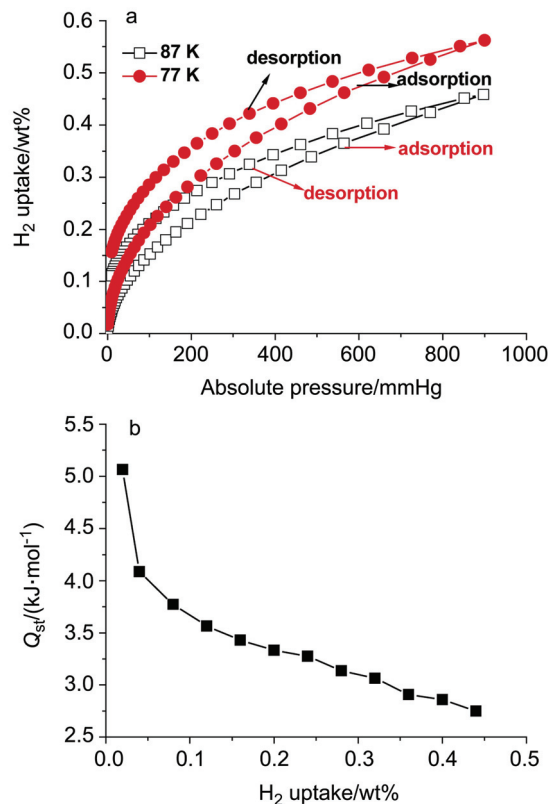


**Figure 5** (a) Adsorption and desorption isotherms of  $\text{H}_2$  at given temperature and low pressure; (b) Isosteric heat of adsorption of  $\text{H}_2$  as function of gas uptake

$\text{CO}_2$  adsorptions at different pressures and different temperatures were also measured. As shown in Figure 7, MWRGO exhibits 7.1 wt%  $\text{CO}_2$  uptake at 1 atm and 273.15 K and that decreases to 4.0 wt% at 303.15 K. Similar to  $\text{H}_2$  adsorption, the higher the pressure, the more uptake of  $\text{CO}_2$ . For example, up to 50.0 wt% was obtained at 273 K and 30 bar. We attribute such high  $\text{CO}_2$  uptake to the large value of the heat of adsorption. At low adsorption amount, the isosteric heat of  $\text{CO}_2$  is nearly 33 kJ/mol, which is comparable to graphene oxide based framework materials and demonstrates strong interaction between  $\text{CO}_2$  and MWRGO.<sup>[36]</sup>

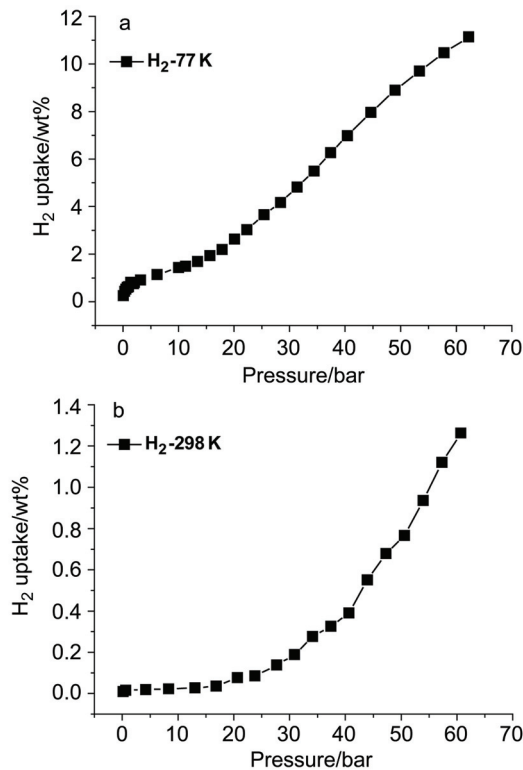


Figure 6 High pressure H<sub>2</sub> adsorption isotherms at 77 K (a) and 298 K (b)

### 3 Conclusion

We have prepared a porous graphene material by reducing GO with MW irradiation. The product has a wrinkled surface and a disordered stacking structure with high SSA and proper pore size for gas storage. It shows a moderate H<sub>2</sub> uptake at 77 K under 1 atm, which is an exciting result considering its relatively low SSA, but high absolute adsorption amount is obtained as pressure increased to 60 bar. The CO<sub>2</sub> storage capacity is 7.1 wt% at ambient conditions. These encouraging results make MWRGO a promising candidate for gas adsorption if we take into consideration the time-saved, large-scale and low-cost preparation procedure. Future work focusing on increasing the specific surface area of MWRGO and its gas storage property is under investigation.

## 4 Experimental

### 4.1 Preparation of MWRGO

GO was prepared from graphite with a particle size of 40 μm (Qingdao Huarun graphite Co., LTD) by the modified Hummers method as described elsewhere<sup>[53]</sup> and is confirmed to be single sheet by atomic force microscope characterization (see SI, Figure S-1). After GO was reduced with the assistance of MW irradiation (DISCOVER, CEM) at the power of 250 W for 1 min in argon environment, well-reduced MWRGO with micropores and mesopores was obtained.

### 4.2 Characterization

In order to investigate the changes in structure, composition and morphology resulted from microwave irradia-

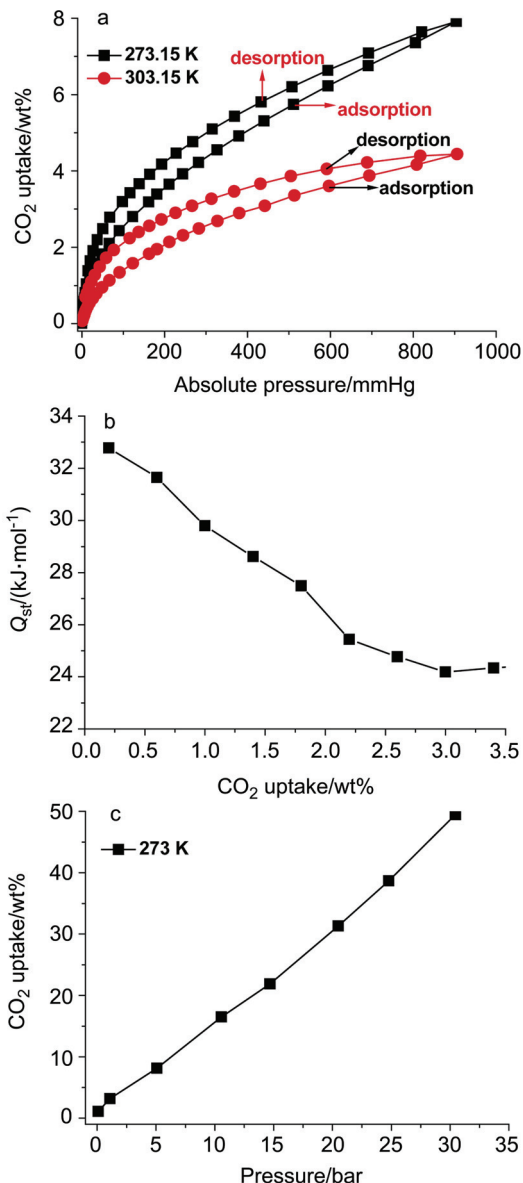


Figure 7 (a) Adsorption and desorption isotherms of CO<sub>2</sub> at given temperature and low pressure; (b) isosteric heat of adsorption of CO<sub>2</sub> as function of gas uptake; (c) High pressure CO<sub>2</sub> adsorption isotherms at 273 K

tion, extensive characterizations were conducted. X-ray diffraction (XRD) measurements were carried out using a Rigaku D/Max-2500 diffractometer with Cu-Kα radiation. Transmission electron microscopy (TEM) characterizations were performed using a Philips T20ST electron microscope at an acceleration voltage of 200 kV. The GO/H<sub>2</sub>O or MWRGO/DMF solution was dropped onto carbon-coated copper grids (mesh size 300) and allowed to dry under ambient conditions. Scanning electron microscope (SEM) measurements were performed on samples as-prepared with Hitachi S-3500N SEM at an acceleration voltage of 20 kV. Thermogravimetric analysis (TGA) was investigated using a NETZSCH STA-409PC instrument with the heating rate of 5 °C/min from room temperature to 900 °C under N<sub>2</sub> atmosphere. Raman spectra were measured with a Renishaw in Via Raman microscope at

room temperature with the 514 nm line of an Ar ion laser as an excitation source. X-ray photoelectron spectra (XPS) were recorded via a Kratos Axis Ultra DLD spectrometer using a monochromatic Al K $\alpha$  X-ray source ( $h\nu=1486.6$  eV), hybrid (magnetic/electrostatic) optics and a multi-channel plate and delay line detector. Infrared spectra were recorded using a Bruker Fourier transform infrared (FT-IR) spectrometer on small pieces of the samples thoroughly mixed with KBr solid while elemental analysis was performed on Yanaca CDRDER MT-3 instrument.

### 4.3 Adsorption investigation

About 80 g MWRCGO was used to evaluate the specific surface area, pore structure, and gas storage properties. The sample cell was firstly evacuated at 125 °C (5 °C/min) for over 12 h before adsorption study was conducted. N<sub>2</sub>, low pressure H<sub>2</sub> and CO<sub>2</sub> adsorption measurements were achieved with a Micromeritics apparatus (ASAP 2020 M). Specifically, N<sub>2</sub> adsorption isotherm was measured under the pressure range of 0~1 atm at 77 K to determine the specific surface area and pore size distribution. Low pressure H<sub>2</sub> adsorption isotherms were measured at 77 and 87 K from 0~900 mmHg while low pressure CO<sub>2</sub> adsorption isotherms were measured at 273 and 303 K. The hydrogen uptake, measured by the gravimetric method at 77 K over the pressure range 1~60 bar were performed using PCTPro-2000.

## References

- [1] Dillon, A. C.; Heben, M. J. *Appl. Phys. A: Mater. Sci. Process.* **2001**, *72*, 133.
- [2] Johnson, J. *Chem. Eng. News* **2004**, *82*, 36.
- [3] Meng, L.-Y.; Park, S.-J. *J. Colloid Interface Sci.* **2010**, *352*, 498.
- [4] Millward, A. R.; Yaghi, O. M. *J. Am. Chem. Soc.* **2005**, *127*, 17998.
- [5] Yong, Z.; Mata, V.; Rodrigues, A. E. *Sep. Purif. Technol.* **2002**, *26*, 195.
- [6] Ma, S.; Zhou, H.-C. *Chem. Commun.* **2010**, *46*, 44.
- [7] Zhu, Y. L.; Long, H.; Zhang, W. *Chem. Mater.* **2013**, *25*, 1630.
- [8] Forster, P. M.; Eckert, J.; Heiken, B. D.; Parise, J. B.; Yoon, J. W.; Jhung, S. H.; Chang, J.-S.; Cheetham, A. K. *J. Am. Chem. Soc.* **2006**, *128*, 16846.
- [9] Liu, C.; Fan, Y. Y.; Liu, M.; Cong, H. T.; Cheng, H. M.; Dresselhaus, M. S. *Science* **1999**, *286*, 1127.
- [10] Zhou, L.; Liu, X. W.; Li, J. W.; Wang, N.; Wang, Z.; Zhou, Y. P. *Chem. Phys. Lett.* **2005**, *413*, 6.
- [11] Yang, Z.; Xia, Y.; Mokaya, R. *J. Am. Chem. Soc.* **2007**, *129*, 1673.
- [12] Fan, Y. Y.; Liao, B.; Liu, M.; Wei, Y. L.; Lu, M. Q.; Cheng, H. M. *Carbon* **1999**, *37*, 1649.
- [13] Wang, H.; Gao, Q.; Hu, J. *J. Am. Chem. Soc.* **2009**, *131*, 7016.
- [14] Lozano-Castello, D.; Lillo-Rodenas, M. A.; Cazorla-Amoros, D.; Linares-Solano, A. *Carbon* **2001**, *39*, 741.
- [15] Yang, J.; Sudik, A.; Wolverton, C.; Siegel, D. J. *Chem. Soc. Rev.* **2010**, *39*, 656.
- [16] Geim, A. K.; Novoselov, K. S. *Nat. Mater.* **2007**, *6*, 183.
- [17] Zhu, Y.; Murali, S.; Cai, W.; Li, X.; Suk, J. W.; Potts, J. R.; Ruoff, R. S. *Adv. Mater.* **2010**, *22*, 3906.
- [18] Bonaccorso, F.; Sun, Z.; Hasan, T.; Ferrari, A. C. *Nat. Photonics* **2010**, *4*, 611.
- [19] Wang, Y.; Shi, Z.; Huang, Y.; Ma, Y.; Wang, C.; Chen, M.; Chen, Y. *J. Phys. Chem. C* **2009**, *113*, 13103.
- [20] Zhang, F.; Zhang, T.; Yang, X.; Zhang, L.; Leng, K.; Huang, Y.; Chen, Y. *Energy Environ. Sci.* **2013**, *6*, 1623.
- [21] Zhang, L.; Zhang, F.; Yang, X.; Long, G.; Wu, Y.; Zhang, T.; Leng, K.; Huang, Y.; Ma, Y.; Yu, A.; Chen, Y. *Sci. Reports* **2013**, *3*, 1408.
- [22] Sui, D.; Huang, Y.; Huang, L.; Liang, J.; Ma, Y.; Chen, Y. *Small* **2011**, *7*, 3186.
- [23] Liang, J.; Huang, L.; Li, N.; Huang, Y.; Wu, Y.; Fang, S.; Oh, J.; Kozlov, M.; Ma, Y.; Li, F.; Baughman, R.; Chen, Y. *ACS Nano* **2012**, *6*, 4508.
- [24] Huang, L.; Yi, N.; Wu, Y.; Zhang, Y.; Zhang, Q.; Huang, Y.; Ma, Y.; Chen, Y. *Adv. Mater.* **2013**, *25*, 2224.
- [25] Patchkovskii, S.; Tse, J. S.; Yurchenko, S. N.; Zhechkov, L.; Heine, T.; Seifert, G. *Proc. Natl. Acad. Sci. U. S. A.* **2005**, *102*, 10439.
- [26] Park, N.; Hong, S.; Kim, G.; Jhi, S.-H. *J. Am. Chem. Soc.* **2007**, *129*, 8999.
- [27] Dimitrakakis, G. K.; Tylianakis, E.; Froudakis, G. E. *Nano Lett.* **2008**, *8*, 3166.
- [28] Tylianakis, E.; Psوفοgiannakis, G. M.; Froudakis, G. E. *J. Phys. Chem. Lett.* **2010**, *1*, 2459.
- [29] Lu, R.; Rao, D.; Lu, Z.; Qian, J.; Li, F.; Wu, H.; Wang, Y.; Xiao, C.; Deng, K.; Kan, E.; Deng, W. *J. Phys. Chem. C* **2012**, *116*, 21291.
- [30] Srinivas, G.; Zhu, Y.; Piner, R.; Skipper, N.; Ellerby, M.; Ruoff, R. *Carbon* **2010**, *48*, 630.
- [31] Ghosh, A.; Subrahmanyam, K. S.; Krishna, K. S.; Datta, S.; Govindaraj, A.; Pati, S. K.; Rao, C. N. R. *J. Phys. Chem. C* **2008**, *112*, 15704.
- [32] Ma, L.-P.; Wu, Z.-S.; Li, J.; Wu, E.-D.; Ren, W.-C.; Cheng, H.-M. *Int. J. Hydrogen Energy* **2009**, *34*, 2329.
- [33] Yang, S.; Zhan, L.; Xu, X.; Wang, Y.; Ling, L.; Feng, X. *Adv. Mater.* **2013**, *25*, 2130.
- [34] Srinivas, G.; Burress, J.; Yildirim, T. *Energy Environ. Sci.* **2012**, *5*, 6453.
- [35] Kumar, R.; Jayaramulu, K.; Maji, T. K.; Rao, C. N. R. *Chem. Commun.* **2013**, *49*, 4947.
- [36] Burress, J. W.; Gadielli, S.; Ford, J.; Simmons, J. M.; Zhou, W.; Yildirim, T. *Angew. Chem.-Int. Ed.* **2010**, *49*, 8902.
- [37] de la Hoz, A.; Diaz-Ortiz, A.; Moreno, A. *Chem. Soc. Rev.* **2005**, *34*, 164.
- [38] Coleman, K. S.; Bailey, S. R.; Fogden, S.; Green, M. L. H. *J. Am. Chem. Soc.* **2003**, *125*, 8722.
- [39] Yan, J.; Fan, Z.; Wei, T.; Qian, W.; Zhang, M.; Wei, F. *Carbon* **2009**, *47*, 3371.
- [40] Sharma, S.; Ganguly, A.; Papakonstantinou, P.; Miao, X.; Li, M.; Hutchison, J. L.; Delichatsios, M.; Ukleja, S. *J. Phys. Chem. C* **2010**, *114*, 19459.
- [41] Zhu, Y.; Murali, S.; Stoller, M. D.; Velamakanni, A.; Piner, R. D.; Ruoff, R. S. *Carbon* **2010**, *48*, 2118.
- [42] Stankovich, S.; Piner, R. D.; Nguyen, S. T.; Ruoff, R. S. *Carbon* **2006**, *44*, 3342.
- [43] Stankovich, S.; Dikin, D. A.; Piner, R. D.; Kohlhaas, K. A.; Kleinhammes, A.; Jia, Y.; Wu, Y.; Nguyen, S. T.; Ruoff, R. S. *Carbon* **2007**, *45*, 1558.
- [44] Okamoto, Y.; Miyamoto, Y. *J. Phys. Chem. B* **2001**, *105*, 3470.
- [45] Subrahmanyam, K. S.; Vivekchand, S. R. C.; Govindaraj, A.; Rao, C. N. R. *J. Mater. Chem.* **2008**, *18*, 1517.
- [46] Sing, K. S. W.; Everett, D. H.; Haul, R. A. W.; Moscou, L.; Pierotti, R. A.; Rouquerol, J.; Siemieniewska, T. *Pure Appl. Chem.* **1985**, *57*, 603.
- [47] Bourlinos, A. B.; Steriotis, T. A.; Karakassis, M.; Sanakis, Y.; Tzitzios, V.; Trapanis, C.; Kouvelos, E.; Stubos, A. *Carbon* **2007**, *45*, 852.
- [48] Du, W. F.; Wilson, L.; Ripmeester, J.; Dutrisac, R.; Simard, B.; Denommee, S. *Nano Lett.* **2002**, *2*, 343.
- [49] Rzepka, M.; Lamp, P.; de la Casa-Lillo, M. A. *J. Phys. Chem. B* **1998**, *102*, 10894.
- [50] Rubes, M.; Bludsky, O. *ChemPhysChem* **2009**, *10*, 1868.
- [51] Xu, W. C.; Takahashi, K.; Matsuo, Y.; Hattori, Y.; Kumagai, M.; Ishiyama, S.; Kaneko, K.; Iijima, S. *Int. J. Hydrogen Energy* **2007**, *32*, 2504.
- [52] Furukawa, H.; Miller, M. A.; Yaghi, O. M. *J. Mater. Chem.* **2007**, *17*, 3197.
- [53] Becerril, H. A.; Mao, J.; Liu, Z.; Stoltenberg, R. M.; Bao, Z.; Chen, Y. *ACS Nano* **2008**, *2*, 463.

(Cheng, B.)